Chapter 17
Palladium-Based Electrocatalysts for Oxygen Reduction Reaction

Minhua Shao

Abstract Fuel cells are clean energy devices that are expected to help address the energy and environmental problems in our society. Platinum-based nanomaterials are usually used as the electrocatalysts for both the anode (hydrogen oxidation) and cathode (oxygen reduction) reactions. The high cost and limited resources of this precious metal hinder the commercialization of fuel cells. Recent efforts have focused on the discovery of palladium-based electrocatalysts with little or no platinum for oxygen reduction reaction (ORR). This chapter overviews the recent progress of electrocatalysis of palladium-based materials including both extended surfaces and nanostructured ones for ORR.

17.1 Introduction

In a low-temperature fuel cell, hydrogen gas is oxidized into protons, electrons, and other by-products when other fuels are used at the anode. At the cathode of the fuel cell, the oxygen is reduced, leading to formation of water. Both the anodic and cathodic reactions require electrocatalysts to reduce the overpotentials and increase reaction rates. In the state-of-the-art low-temperature fuel cells, Pt-based materials are used as the electrocatalysts for both the reactions; however, the high cost and limited resources of this precious metal are hindering the commercialization of fuel cells. Recent efforts have focused on the discovery of electrocatalysts with little or no Pt for oxygen reduction reaction (ORR) [1–3].

The electrocatalytic activity of Pd is the second highest among the pure metals for ORR, only behind Pt. This, combined with the fact that the cost of Pd is lower than that of Pt, makes it an attractive alternative to Pt. Figure 17.1 compares the prices per troy ounce of Pd and Pt in the last 10 years [4]. The cost of Pd is roughly

M. Shao (✉)
UTC Power, 195 Governor's Highway, South Windsor, CT 06074, USA
e-mail: minhua@gmail.com

M. Shao (ed.), *Electrocatalysis in Fuel Cells*, Lecture Notes in Energy 9,
DOI 10.1007/978-1-4471-4911-8_17,

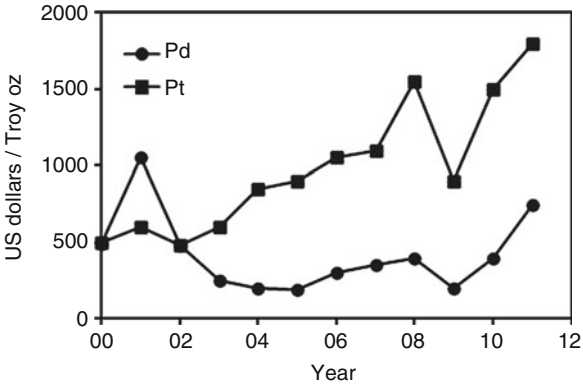

Fig. 17.1 Comparison of the cost of Pd and Pt per troy ounce in the period of 2000–2011

one quarter of Pt except in the period of 2000–2002 when it spiked to $1,100 per troy oz due to insufficient supply in the market. Similar to Pt, most Pd today is used in the automotive industry for catalytic converters to reduce the toxicity of emissions from a combustion engine.

While Pd is less expensive than Pt, the electrocatalytic activity of bulk polycrystalline Pd for ORR is at least five times lower than that of Pt, which prevents it from being used directly in fuel cells. Great efforts have been dedicated to improve the activity of Pd by surface modification and alloying. This chapter attempts to summarize the recent progress of electrocatalysts containing Pd for ORR. The development of Pd electrocatalysts for electrooxidation of hydrogen and small organic molecules is not discussed in this chapter but has been adequately covered in Chaps. 5 and 6 and recent reviews [5–7].

17.2 ORR in Acid Solutions

17.2.1 ORR on Bulk Surfaces

Due to its complexity, the ORR mechanisms on noble metal surfaces are not fully understood despite five decades' extensive studies [8–10]. On Pt surfaces, it is generally accepted that the first electron transfer or oxygen adsorption together with an electron and proton transfer forming superoxide (Eq. 17.1) is the slow step determining the overall reaction rate of oxygen reduction:

$$O_2 + H^+ + e^- \rightarrow OOH_{ads}. \tag{17.1}$$

It is reasonable to assign (Eq. 17.1) to the rate-determining step of ORR since it requires a significant energy to form a bond between Pt and oxygen before the O–O can break. This assignment has been supported by recent experimental and

theoretical work. One may agree that a reactive surface facilitates the reaction (Eq. 17.1), i.e., the more reactive the surface, the stronger the oxygen bond. The O–O bond dissociation generates adsorbed OH species, which need to be further reduced to complete the four-electron reaction according to

$$OH_{ads} + H^+ + e^- \rightarrow H_2O. \tag{17.2}$$

Unlike Eq. (17.1), the strong adsorption of OH on catalyst surfaces hinders its reduction and hence slows down the ORR rate. In addition, the buildup coverage of oxygen-containing species decreases the availability of active surface sites. Thus, a good ORR catalyst is one that forms a moderate bond with the adsorbates to balance the kinetics of O–O bond breaking and removal of oxygen-containing species generated from the former step. Density functional theory (DFT) calculations demonstrated that the oxygen binding energy (BEo) on Pt(111) is a little bit too strong and Eq. (17.2) is the bottleneck of the ORR. If slightly weakened, such as found for a surface of Pt monolayer on Pd(111) (denoted as Pt/Pd(111)) [11] and for a Pt skin on various Pt alloys [12–14], the ORR activity can be enhanced remarkably.

Pd is a more reactive metal than Pt and binds oxygen more strongly. It oxidizes at more negative potentials than Pt and is expected to be less active for ORR [15]. The study of ORR on Pd bulk electrodes in acidic media has received less attention than on Pt due to the lower activity and stability of the former. The first direct comparison of ORR activity between polycrystalline Pd and Pt was attempted by Damjanovic and Brusic [16], who found that the exchange current densities for a polycrystalline Pd and Pt electrode were 2×10^{-11} and 10^{-10} A cm^{-2}, respectively, in a $HClO_4$ solution. In other words, the bulk Pt is five times more active than Pd in this study. It has been well known that the ORR kinetics strongly depends on the electrolyte used in the experiment and on the crystallographic orientation of the electrodes. For instance, the ORR activity of low index planes of Pt follows the order of Pt(111) < Pt(110) < Pt(100) in H_2SO_4 solutions. While in $HClO_4$ solutions, it follows the order of Pt(100) < Pt(111) ≤ Pt(110) [17]. The main reason for the lower activity of Pt(111) than Pt(100) in H_2SO_4 solutions is the much stronger adsorption of SO_4^{2-} and HSO_4^- on the former. On the other hand, there is no anion strongly adsorbed on either surface in the $HClO_4$ solutions. In such electrolytes, the discrepancy of the activity on the different surfaces originates primarily from the structural and electronic properties of the surfaces rather than from the poisoning effect from specific adsorption of the anions.

Due to the difficulty of preparing Pd single crystals and their poor stability, the facet-dependent ORR activities of the Pd single crystals have not been available until very recently. Kondo et al. [18] measured the ORR activities of low index planes of Pd single crystals in $HClO_4$ solution and found that the activity increased following the order of Pd(110) < Pd(111) ≪ Pd(100). This order is completely opposite to that on Pt(hkl) in the same solution. The comparison of the kinetic activities on different Pd and Pt facets is shown in Fig. 17.2. Surprisingly, the

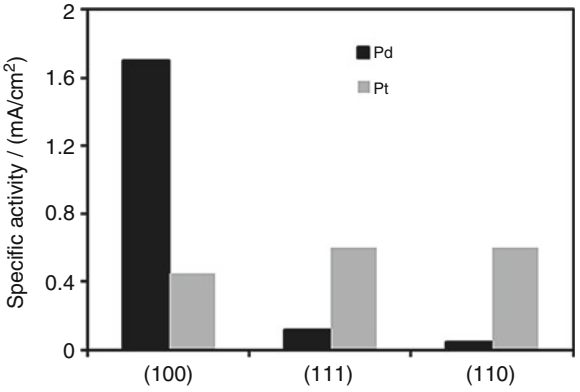

Fig. 17.2 Comparison of specific activity of oxygen reduction on low index facets of Pd and Pt single crystals at 0.9 V [18]

activity of Pd(100) is 14 times as high as that of Pd(111). It is also worth noting that Pd(100) is even more active than Pt(111). The kinetic current densities of ORR correlate well with the terrace atom density on *n*(100)-(111) and *n*(100)-(110) series of Pd suggesting that (100) atoms are the most active sites for ORR on Pd electrodes. Further fundamental studies are needed to understand the mechanisms of facet dependence of ORR activity on Pd(hkl). Recent DFT study revealed a dramatic difference in reactivity between the Pd(111) and (100) surfaces. The Pd–O bond on Pd(100) surface is weaker than that on Pd(111) by 0.04 eV. As discussed above, the Pd(111) binds to the oxygen intermediates too strongly resulting in a low ORR activity. A weaker Pd–O bond on (100) may explain its superior ORR activity.

According to d-band center theory, one way to improve the ORR kinetics of Pd surfaces is to reduce the BEo by lowering its d-band center. The DFT calculations reported by Shao et al. [19] revealed that the Pd monolayer on Pt(111) has a lower d-band center than a bare Pd(111) surface and hence a lower BEo, making Pd/Pt (111) a better catalyst than Pd(111) for ORR. This argument was supported by their experimental work, which showed that Pd/Pt(111) had a higher ORR activity than Pd(111), but somewhat lower than Pt(111) [19].

17.2.2 ORR on Pd-Based Nanocatalysts

By alloying Pt with transition metals M (M = V, Cr, Co, Ni, Fe, Ti, etc.), the ORR activity can be enhanced remarkably in both phosphoric acid fuel cell (PAFC) and PEMFC [20–22]. The activity enhancement mechanisms have been an open question for more than three decades and ascribed to decreased Pt–Pt bond distance [23], enhanced surface roughness [24], increased Pt d-band vacancy [25–27], weakened OH adsorption [28, 29], and downshifted d-band center [30–35]. Nørskov and Mavrikakis et al. combined the structural and electronic effects by introducing a d-band model that correlates changes in the energy center of the valence d-band density of states at the surface sites with their ability to form chemisorption bonds.

According to their model, the binding energy of oxygen-containing species on Pt skin formed during selective leaching of non-noble metals or annealing at high temperatures was weaker than on a pure Pt surface due to the compressive strain and electron transfer from the transition metal on the subsurface layer. Similar to Pt, the activity of Pd can be enhanced by alloying with transition metals.

17.2.2.1 Binary Pd Alloy Catalysts

Savadogo's group was the first to discover the enhanced ORR activities on Pd alloys [36]. It was found that Pd–Co, Ni, and Cr bulk alloys prepared by sputtering had higher activity than Pt prepared in a same way in acidic solutions. Since their groundbreaking results, many groups have reported the oxygen reduction behaviors of various Pd alloys. Bard's group [37–39] identified a series of Pd-based catalysts, including binary systems Pd–Co, Mn, V, and Ti, that showed higher ORR activity than pure Pd. For Pd–Co/C, the maximum activity was observed with a Co atomic ratio in the range of 10–20 %, but the high activity was lost quickly during electrochemical testing, maybe due to the fast dissolution of Co atoms [38]. One would expect that the dissolution rate of Co in Pd–Co alloy is much faster than that in Pt–Co.

The compositions of Pd alloys play an important role in ORR activity. Depending on the synthesis methods and annealing temperatures, different optimum Pd:M ratios for ORR were reported. Shao et al. [19] found that Pd_2Co/C synthesized by the impregnation method and annealed at 900 °C exhibited the highest ORR activity. The same optimum ratio was also observed by Wang et al. [40], who co-reduced Pd and Co salts in ethylene glycol and annealed the dried product at 500 °C. The highest ORR activity for Pd–Co catalysts (30–40 at.% Co), formed by co-reducing Pd and Co salts in aqueous solutions, was obtained by Zhang et al. [41]. Particle size, as well as the activity, increased with increasing annealing temperature, and the highest activity was observed at the lowest annealing temperature (300 °C). For the Pd–Fe systems, an optimized composition of Pd:Fe = 3:1 was found by several groups [42–45]. The ORR activity of Pd_3Fe/C was comparable to or higher than that of Pt/C. The activity was found to correlate well with the Pd–Pd bond distance and the Fe content in the alloy (Fig. 17.3) [42, 46]. The highest ORR activity was obtained for Pd_3Fe, which has a Pd–Pd bond distance of 0.273 nm, smaller than that of Pd by 2.3 %. Similar results were obtained for the Pd–Co alloys [40], suggesting the compressed lattice plays a role in the activity enhancement. The activity of Pd_3Fe was found to be further enhanced by adding a small amount of Ir in it [43]. The enhancement mechanism is unknown. For Pd–W alloys annealed at 800 °C, only 5 % W is needed to maximize the activity [47].

Oxygen reduction activities of some Pd–nonmetallic element alloys (Pd–Se, S, and P) were also studied, but no significant improvements have been observed [48, 49]. Pd–Pt alloys, however, showed higher ORR activity than Pt with a small amount of Pd in the alloys. For instance, Li et al. found that Pt–Pd/C exhibited a slightly higher ORR activity than Pt/C [50]. Guerin et al. found that the Pd–Pt alloys showed higher

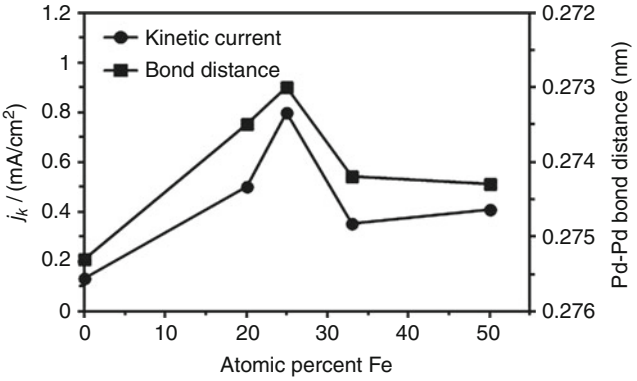

Fig. 17.3 Specific activity and Pd–Pd bond distance calculated from XRD data against the concentration of Fe in Pd–Fe/C electrocatalysts. All samples were treated at 500 °C [42]

activity than Pt in a composition range of 70–90 % Pt [51]. The high activity was also observed on dendrimer-encapsulated Pd–Pt nanoparticles containing 180 atoms with a Pt:Pd ratio of 5:1 [52]. The enhanced activity may be explained by a shorter Pt–Pt bond distance.

17.2.2.2 Ternary Pd Alloy Catalysts

Most of the binary alloys have limited durability. By incorporating a more corrosion-resistant metal, like Au, Mo, and Mn, the stability of the alloy was enhanced significantly [37, 53]. For example, Pd–Co–Mo catalysts with a Pd:Co:Mo atomic ratio of 70:20:10 exhibited not only higher activity than Pt/C but with excellent chemical stability during fuel cell testing [53]. Other Pd–Co–M (M = Pt, Au, Ag) ternary catalysts have been investigated by Mathiyarasu and Phani [54]. As expected, the Pd–Co–Pt combination showed the highest activity which was higher than Pt/C, but Pd–Co and Pd–Co–Au exhibited very low activity, which is contrast to other reports [19, 37].

17.2.2.3 Synthesis and Particle Size Effect

The activity discrepancy for Pd-based catalysts with similar compositions has been seen in the literature. One of the main reasons is that the properties of the Pd alloys highly depend on the synthesis method and posttreatment. A good example is the Pd–Cu system. Wang et al. [55, 56] found that $PdCu_3$ catalysts synthesized by a colloidal method showed a higher activity than those made by thermodecomposition, benefiting from the more uniform alloying and much smaller particle size in the former method. Raghuveer et al. [57] also concluded that the activity

of Pd–Co–Au synthesized by the microemulsion method was higher than that prepared by the conventional sodium borohydride reduction method due to the smaller particle size and higher degree of alloying.

The effects of particle size and degree of alloying were studied by Liu and Manthiram in the $Pd_{70}Co_{30}$/C catalysts [58]. Upon increasing the annealing temperature from 350 to 500 °C, the catalytic activity decreased due to increasing the alloying degree and particle size. Further increasing the annealing temperature resulted in further activity decreases, though this was attributed solely to the increase in particle size. An interesting trend is that the activity of Pd–Co alloy decreased with increasing the degree of alloying in the case of the same particle size. It seems that high Co content is not necessary for activity improvement. Further study is needed to understand the role of alloying degree and transition metal contents by controlling the particle size and compositions. Due to the high surface energy of Pd, it is very difficult to synthesize monodispersed Pd–M (M = transition metals) nanoparticles with small particle size. Such study requires novel synthesis method of Pd alloys.

17.2.2.4 Structural Effect

The ORR activity of Pd-based catalysts depends on the shape and morphology of the materials. Pd(100) exhibited the highest ORR activity among the low index facets [18]. Several studies reported the shape-dependent ORR activities in nanoscale materials. The specific activity of Pd nanorods prepared by Xiao et al. [59] was ten times higher than that of Pd nanoparticles and comparable to that of bulk Pt. The authors attributed the high activity to the contribution from (110) sites according to their DFT calculations, which is in contrast to what was observed in the single-crystal work [18]. Li et al. [60] synthesized PdFe nanorods with a diameter of 3 nm and length of 10–50 nm, which can be controlled by the amount and type of surfactants. The PdFe nanorods demonstrated a higher PEMFC performance than commercial Pt/C in the practical working voltage region (0.80–0.65 V). The electrocatalytic activities of other shape-controlled Pd-based nanomaterials (cubic, octahedral, nanowires, etc.) are also of interest.

Erikson et al. demonstrated that cubic Pd particles enriched with {100} facets with an average size of ~27 nm had a higher ORR activity than spherical Pd particles (2.8 nm) [62]. A systematic study on the structural dependence of electrochemical behavior of Pd nanocrystals with a much smaller particle size (5–6 nm) was reported by Shao et al. [63]. As shown in Fig. 17.4a, the hydrogen adsorption peaks were observed at 0.16 and 0.21 V for the Pd cubes and octahedra, respectively [61]. The peak for the Pd cubes was sharper than that for the Pd octahedra. The differences in position and shape of hydrogen peaks may be caused by a weaker adsorption of hydrogen on Pd(100) than that on Pd(111). The differencebetween Pd cubes and octahedral was also confirmed by their Cu underpotential deposition (UPD) curves (Fig. 17.4b) [61]. For Pd octahedra, a sharp current peak was observed at 0.51 V due to UPD of Cu on {111} facets. On the other hand, a broader

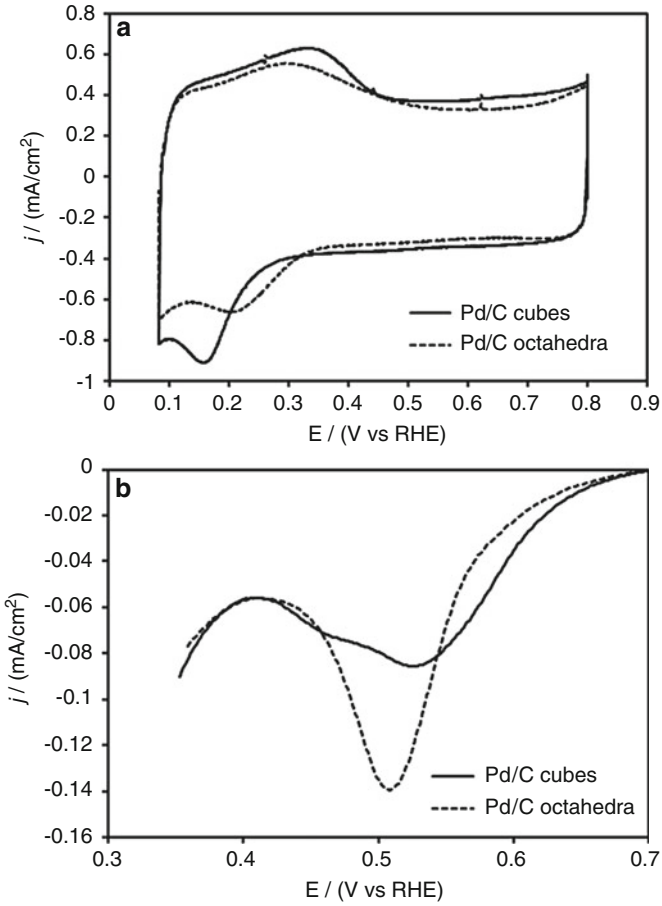

Fig. 17.4 Cyclic voltammetry curves of carbon-supported Pd nanocrystals. (**a**) In a nitrogen-saturated 0.1 M $HClO_4$ solution. Scanning rate = 50 mV s^{-1}. (**b**) In a nitrogen-saturated 0.05 M H_2SO_4 + 0.05 M $CuSO_4$ solution. Scanning rate = 5 mV s^{-1}. The double-layer currents were subtracted from the Cu UPD curves [61]

peak appeared at ca. 0.54 V for Pd cubes due to UPD of Cu on {100} facets. The higher Cu UPD potential on {100} than on {111} facets is due to a larger difference in work function between Pd(100) and Cu(100) than that between Pd (111) and Cu(111) and is consistent with the results obtained from bulk single crystals [64].

The oxygen polarization curve of Pd/C cubes is much more positive compared to those of octahedral and conventional Pd/C (Fig. 17.5a). This indicates that the Pd/C cubes were much more active for oxygen reduction. The specific ORR activities of Pd atoms in different samples were compared in the inset of Fig. 17.5a. The specific activities of cubic, octahedral, and conventional Pd/C were 0.31, 0.033, and 0.055 mA cm^{-2}, respectively. The activity enhancement of Pd cubes was about

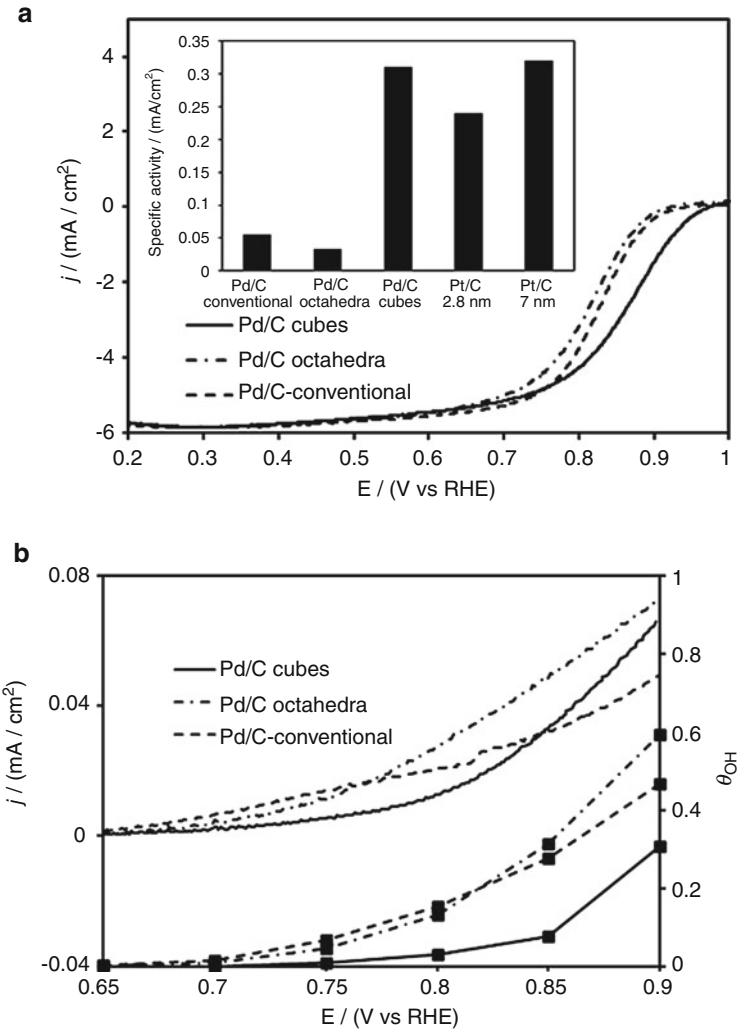

Fig. 17.5 (**a**) Anodic polarization curves for the ORR on Pd cubes and octahedra supported on carbon black in 0.1 M $HClO_4$. The data of conventional Pd/C is also included for comparison. Sweep rate = 10 mV s^{-1}; rotating speed = 1,600 rpm; and room temperature. The currents were normalized to the geometric area of the rotating disk electrode. The electrochemically active areas of Pd/C cubes, Pd/C octahedra, and Pd/C-HT were 1.27, 1.4, and 0.98 cm^2, respectively. *Inset*: comparison of specific activities for Pd/C cubes, Pd/C octahedra, conventional Pd/C, Pt/C (2.8 nm), and Pt/C (7 nm) at 0.9 V. (**b**) Anodic polarization curves in 0.1 M $HClO_4$ and coverage of OH of Pd/C cubes, Pd/C octahedra, and conventional Pd/C after subtracting the double-layer current density. The currents were normalized to the electrochemical active area. The coverage of OH was calculated by integrating the charge associate with OH_{ad} formation and normalized to half of the charge of Cu UPD [63]

ten and six times over Pd/C octahedra and conventional Pd/C, respectively. The Pd/C cubes were even more active than the state-of-the-art Pt/C catalysts with an average particle size of 2.8 nm and comparable to Pt/C with a similar particle size. This result demonstrated that Pd(100) sites are much more active than Pd(111) at the nanoscale, consistent with the extended surface study.

The ORR kinetics is controlled by the amount of available active sites on the catalyst's surface and the interaction between the surface and oxygen-containing species (e.g., O_2, O, OH, and OOH). The chemisorbed OH (OH_{ad}) acts as a poison species in the potential range where oxygen reduction is under combined kinetic–diffusion control, since it blocks the surface sites for O_2 adsorption. Shao et al. [63] compared the anodic branches of the voltammetry curves (0.65–0.9 V) for cubic, octahedral, and conventional Pd/C after subtracting the double-layer currents (Fig. 17.5b). The onset potential of OH_{ad} formation for both octahedral and conventional Pd was more than 50 mV lower than Pd cubes. Consequently, the coverage of OH_{ad} (Θ_{OH}) on Pd cubes was much lower than other surfaces in the potential range > 0.7 V. Thus, the higher ORR activity on Pd cubes can be attributed to its lower OH_{ad} coverage and consequently more available reaction sites.

17.3 ORR in Alkaline

17.3.1 ORR on Bulk Surfaces

The development of alkaline fuel cells promotes the studies of ORR on Pd-based materials in alkaline medium. A four-electron transfer reaction is expected on Pd surfaces:

$$O_2 + 2H_2O + 4e^- \rightarrow 4OH^-. \tag{17.3}$$

Lima et al. studied the ORR activities of different noble metals with a {111} facet in a 0.1 M NaOH solution [65]. The results showed that Pd(111) was more active in an alkaline solution than in an acidic solution, with an ORR activity very close to that of Pt(111) in the former solution.

Arenz et al. found that Pd/Pt(111) has a higher ORR activity than Pt(111) in alkaline solution, which is different from that in acid solution [66]. In alkaline solution, where only OH anions are present, the inhibition effect from the strong anion adsorption is much smaller than in acidic solution, resulting in a high ORR activity. Pd overlayers on Au(100) and Au(111) also showed significant activity improvement with respect to an unmodified Au substrate in the alkaline solutions [67–69]. The very high activity of Pd in alkaline solutions is surprising and deserves further attention.

17.3.2 ORR on Pd-Based Nanocatalysts

Pd exhibits a higher ORR activity in alkaline than in acidic solutions due to a decrease in the anion poisoning effect in alkaline solutions. Indeed, many studies have shown that the ORR activity of Pd/C in alkaline solutions is comparable to that of Pt/C [70, 71]. Similar to that of Pt/C, the ORR activity of Pd/C is dependent on the particle size of the metal. Jiang et al. [71] demonstrated that the specific activity increased monotonically by a factor of about 3 with the particle size increasing from 3 to 16.7 nm, while the mass activity first increased when the Pd particle size increased from 3 to 5 nm and then decreased with further Pd particle size increases. The increase of the specific activity is contributed to the increase of the fraction of the facet atoms with increasing the particle size.

The ORR activities of Pd–M alloys (M = Fe, Ni, Au, Sn) [70, 72–74] have also been studied in alkaline solutions. The Pd_3Fe/C was twofold more active than pure Pd/C [70]. Similar activity enhancement was also observed on Pd–Sn alloys [72]. For Pd–Ni/C catalyst, the ORR activity depends on the composition of the alloys. The highest activity was observed on PdNi/C and Pd_3Ni/C, which was not superior to Pd/C or Pt/C [73]. A synergistic effect from WC on ORR activity has been observed by Ni et al. [74]. The Pd nanoparticles supported on WC/C synthesized by an intermittent microwave heating method showed an enhanced ORR activity in comparison to Pd/C and Pt/C. By alloying with Au, the activity of Pd was significantly enhanced, but the exact enhancement mechanism is not clear. The strong interaction between the supports and metal nanoparticles and its effect on ORR activity may be an interesting topic to study. The development of Pd-based ORR catalysts for alkaline fuel cells is of interest to replace costly Pt materials. The ORR activity and stability of Pd-based catalysts, however, has to be compared to that of less expensive non-precious metal electrocatalysts [75, 76].

17.4 Methanol Tolerance

One of the main issues in the direct alcohol fuel cells (DAFCs) is that the fuel can easily permeate into the cathode through the proton exchange membrane, which causes dramatic performance loss since the currently used Pt-containing cathode catalysts have no or little methanol tolerance. One of the advantages of Pd–M alloys over Pt in DAFCs is their high methanol and ethanol tolerance in acid. In particular, methanol tolerance was demonstrated for Pd–Fe, Pd–Co, Pd–Cr, Pd–Ni, and Pd–Pt alloys [19, 41, 53, 77–80].

Shao et al. found no evidence of methanol oxidation on Pd_2Co/C in nitrogen-saturated $HClO_4$ solution containing 0.1 M methanol (Fig. 17.6) [19]. For the ORR, the half-wave potential drops ca. 20 mV with 0.1 M methanol in solution, compared to the same electrocatalyst without methanol. The loss of 20 mV might reflect the blocking of some active sites for oxygen reduction by the adsorbed methanol or its intermediates from oxidation. Similar methanol tolerance properties of Pd–M

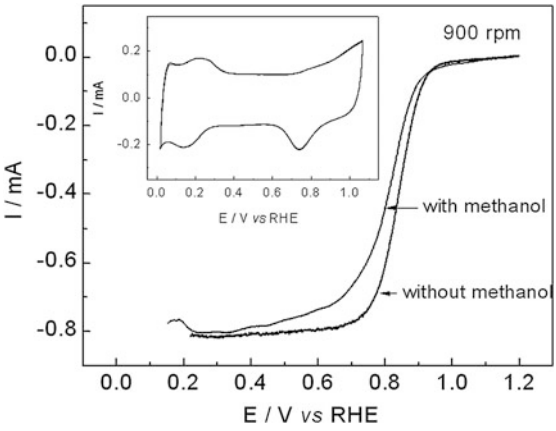

Fig. 17.6 Comparison of polarization curves for ORR on Pd_2Co/C in oxygen-saturated 0.1 M $HClO_4$ solution with and without 0.1 M methanol; rotation rate 900 rpm; sweep rate 10 mV s^{-1}. The *inset* is the cyclic voltammetry of Pd_2Co/C nanoparticles in nitrogen-saturated 0.1 M $HClO_4$ + 0.1 M methanol solutions; sweep rates 20 mV s^{-1} [19]

alloys have been reported by numerous groups [41, 77, 80–82]. All the results confirmed the excellent methanol tolerance of Pd-based alloys due to the low methanol oxidation on these electrocatalysts. By alloying with Pd, the methanol tolerance of Pt-based catalysts can be improved by diluting the Pt–Pt bonds, which are required for dissociative adsorption of methanol and ethanol on the surface of the catalyst. Accordingly, both Pd–M and Pd–Pt catalysts might be good candidates for resolving the problem of methanol crossover in DMFCs.

17.5 Mechanism of ORR Activity Enhancement

An understanding of the origin of the high activities of Pd–M alloys may help us in designing inexpensive and more active catalysts. Some thermodynamic guidelines were proposed to understand the enhancement effect from the alloying with transition metals. Bard and coworkers [38, 39] suggested that for Pd–M alloys the reactive metal M constitutes the site for breaking the O–O bonds, forming O_{ads} that would migrate to the hollow sites dominated by Pd atoms, where it would be readily reduced to water. Based on this mechanism, the alloy surface should consist of a relatively reactive metal such as Co, and the atomic ratio of this metal should be 10–20 % so that there are sufficient sites for reactions of O–O bond breaking on M and O_{ads} reduction at hollow sites formed by Pd atoms. The DFT calculations [39] indicated that one of the O atoms diffused to the Pd hollow site while the other still adsorbed on the hollow site near Co after the dissociative adsorption of the O_2 molecule. The second O_2 could dissociate on Co with an O atom prebound on the hollow site near it. Balbuena et al. [83] and Savadogo et al. [84] proposed a similar thermodynamic guideline for designing Pd alloy catalysts. For Pd with fully occupied valence d-orbitals, alloying with transition metals, such as Co with unoccupied valence d-orbitals, significantly reduces the Gibbs free energy both for the first charge-transfer step and for the steps involving the reduction of intermediates.

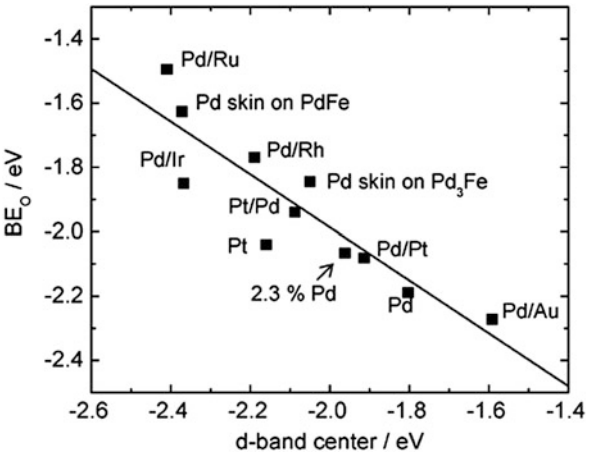

Fig. 17.7 Calculated oxygen binding energies on Pd and Pt overlayers on various substrates as a function of the Pd d-band center (relative to the Fermi level). The energies plotted correspond to the most stable configuration for O adsorption at the Pd or Pt hollow sites on each surface [89]

A Pd-enriched surface or called Pd skin can be formed either by annealing at elevated temperatures [85–87] or potential cycling before ORR activity evaluation. DFT calculations show that, like the Pt_3Co alloy surfaces, the electronic structure of the Pd skin is modified by the compressive strain (the transition metals used in the Pd alloys usually have a smaller atomic radius than that of Pd) and the underlying alloy, which in turn modifies the reactivity of the surface [88, 89]. As shown in Fig. 17.7, compressive strain alone accounts for a 0.1 eV destabilization of the Pd–O bond. A $Pd_3Fe(111)$ substrate contributes a further destabilization of O by ca. 0.25 eV, whereas a PdFe(111) substrate contributes a further destabilization of O by ca. 0.35 eV. The Pd skin on $Pd_3Fe(111)$ is very similar to Pt(111) in terms of both the d-band center position and the oxygen binding energy, and should have a high ORR activity. The high activity of this alloy was confirmed by using a $Pd_3Fe(111)$ single crystal by Zhou et al. [90].

17.6 Durability of Pd-Based Electrocatalysts

The durability of low-temperature fuel cell is one of the essential topics in the fuel cell development. The fuel cell performance gradually decreases due to the degradation of the Pt-based catalyst l under the harsh operating conditions including high potential, low pH, high temperature, and frequent start–stop cycling [2, 91]. The thermodynamic behavior of bulk Pt is described by the potential–pH diagrams (Pourbaix diagrams) [92]. The main pathways for Pt dissolution involve either the direct dissolution of metal,

$$\mathrm{Pt} \rightarrow \mathrm{Pt}^{2+} + 2\mathrm{e}^- \quad E_0 = 1.19 + 0.029 \log\left[\mathrm{Pt}^{2+}\right], \tag{17.4}$$

or an oxide film formation and a subsequent chemical reaction,

$$\mathrm{Pt} + \mathrm{H_2O} \rightarrow \mathrm{PtO} + 2\mathrm{H^+} + 2\mathrm{e^-} \quad E_0 = 0.98 - 0.59\,\mathrm{pH}, \tag{17.5}$$

$$\mathrm{PtO} + 2\mathrm{H^+} \rightarrow \mathrm{Pt^{2+}} + \mathrm{H_2O} \quad \log[\mathrm{Pt^+}] = -7.06 - 2\,\mathrm{pH}. \tag{17.6}$$

The dissolution through Pt oxides is expected to be slow due to the self-passivation effect. Similar to Pt, Pd can dissolve in acid solution via [92]

$$\mathrm{Pd} \rightarrow \mathrm{Pd^{2+}} + 2\mathrm{e^-} \quad E_0 = 0.99 + 0.029\,\log\left[\mathrm{Pd^{2+}}\right], \tag{17.7}$$

or

$$\mathrm{Pd} + \mathrm{H_2O} \rightarrow \mathrm{PdO} + 2\mathrm{H^+} + 2\mathrm{e^-} \quad E_0 = 0.90 - 0.59\,\mathrm{pH}, \tag{17.8}$$

$$\mathrm{PdO} + 2\mathrm{H^+} \rightarrow \mathrm{Pd^{2+}} + \mathrm{H_2O} \quad \log[\mathrm{Pd^+}] = -2.35 - 2\,\mathrm{pH}. \tag{17.9}$$

In the direct dissolution pathway, the equilibrium potential of Pd dissolution is 0.2 V lower than that of Pt. In the chemical dissolution pathway, the Pd^{2+} equilibrium concentration is ~5 orders of magnitude higher than Pt^{2+}. Thus, Pd should have a much higher dissolution rate at the same operation potential and thus much less stable than Pt in the fuel cell environment. Consequently, Pd is not expected to meet the durability requirement of the PEMFC, especially for those in the automotive application due to intensive start–stop driving cycles. The very low stability of Pd/C during potential cycling was confirmed recently [93]. The stability of Pd in alkaline medium may not be a problem; however, no such study is available in the literature.

Considerable efforts have been taken to improve the stability of Pd-based catalysts in the acidic medium. One way is to alloy with certain elements. Pd ternary alloys, including Pd–Co–Au [38, 39] and Pd–Co–Mo [53], have been developed to improve the stability of the catalysts. By adding 10 % Au to the Pd–Mo mixture, its stability can be improved significantly. However, the long-term durability of these catalysts has not been addressed yet.

Another promising way to improve the activity and durability of Pd-based nanocatalysts is to deposit a Pt layer on them. Recently, Pd/C and PdM/C catalysts modified by a Pt monolayer were found to possess higher activity than that of Pt/C due to the strain and electronic effects from the Pd-based cores, and the durability of the catalysts is improved significantly and comparable to Pt/C [70, 93–95]. The Pd-based core materials are expected to be partially dissolved under the fuel cell operation conditions due to some defects in the Pt monolayer. In the meantime, the diffusion of Pt atoms on the surface results in a more compact shell. Thus, further dissolution of Pd-based core is greatly reduced.

17.7 Conclusions

Pd-based electrocatalysts have shown comparable ORR activity to state-of-the-art Pt/C. It may play a role to replace or partially replace costly Pt catalysts in the cathode of low-temperature fuel cells.

As expected, the oxygen reduction rate strongly depends on the orientations of the Pd surface with Pd(100) having a much higher ORR activity than any other facets in acid. This trend has been confirmed both in the studies of bulk single crystals and nanocrystals of Pd. Synthesis and characterization of shape-controlled Pd and Pd alloy nanomaterials are of importance to design next generation Pd-based electrocatalysts.

The long-term stability of Pd-based electrocatalysts is one of the unavoidable issues for PEM fuel cell applications. Pd–Pt-based ORR catalysts are more stable than Pd-transition metal alloys under harsh fuel cell conditions, but may still not meet the long-term fuel cell operation requirement due to the Pd leaching out. Future research may focus on improving the durability of Pd-based catalysts by surface modification and composition optimization. Core–shell type of catalyst with Pd-based materials as the core and Pt as the shell may be one of the most promising candidates to be used in the automotive fuel cell due to its low Pt content and high activity and stability.

References

1. Adzic RR, Zhang J, Sasaki K, Vukmirovic MB, Shao M, Wang JX, Nilekar AU, Mavrikakis M, Valerio JA, Uribe F (2007) Platinum monolayer fuel cell electrocatalysts. Top Catal 46(3–4): 249–262
2. Gasteiger HA, Kocha SS, Sompalli B, Wagner FT (2005) Activity benchmarks and requirements for Pt, Pt-alloy, and non-Pt Oxygen reduction catalysts for PEMFCs. Appl Catal B Environ 56(1–2):9–35
3. Lefevre M, Proietti E, Jaouen F, Dodelet JP (2009) Iron-based catalysts with improved oxygen reduction activity in polymer electrolyte fuel cells. Science 324(5923):71–74
4. www.monex.com
5. Antolini E (2009) Palladium in fuel cell catalysis. Energy Environ Sci 2(9):915–931
6. Bianchini C, Shen PK (2009) Palladium-based electrocatalysts for alcohol oxidation in half cells and in direct alcohol fuel cells. Chem Rev 109(9):4183–4206
7. Shao M (2011) Palladium-based electrocatalysts for hydrogen oxidation and oxygen reduction reactions. J Power Sources 196(5):2433–2444
8. Adzic RR (1998) Electrocatalysis. In: Lipkowski J, Ross PN (eds) Frontiers in electrochemistry, vol 5. Wiley, New York, p 197
9. Shao MH, Liu P, Adzic RR (2006) Superoxide is the intermediate in the oxygen reduction reaction on platinum electrode. J Am Chem Soc 128:7408–7409
10. Tarasevich MR, Sadkowski A, Yeager E (1983) Oxygen electrochemistry. In: Conway BE, Bockris JO, Yeager E, Khan SUM, White RE (eds) Comprehensive treatise of electrochemistry, vol 7. Plenum, New York, p 301

11. Zhang J, Vukmirovic MB, Xu Y, Mavrikakis M, Adzic RR (2005) Controlling the catalytic activity of platinum-monolayer electrocatalysts for oxygen reduction with different substrates. Angew Chem Int Ed 44:2132–2135
12. Xu Y, Greeley J, Mavrikakis M (2005) Effect of subsurface oxygen on the reactivity of the Ag(111) surface. J Am Chem Soc 127(37):12823–12827
13. Stamenkovic V, Mun BS, Mayrhofer KJJ, Ross PN, Markovic NM, Rossmeisl J, Greeley J, Nørskov JK (2006) Changing the activity of electrocatalysts for oxygen reduction by tuning the surface electronic structure. Angew Chem Int Ed 45(18):2897–2901
14. Stamenkovic VR, Fowler B, Mun BS, Wang G, Ross PN, Lucas CA, Markovic NM (2007) Improved oxygen reduction activity on $Pt_3Ni(111)$ via increased surface site availability. Science 315:493
15. Norskov JK, Rossmeisl J, Logadottir A, Lindqvist L, Kitchin JR, Bligaard T, Jonsson H (2004) Origin of the overpotential for oxygen reduction at a fuel-cell cathode. J Phys Chem B 108: 17886–17892
16. Damjanovic A, Brusic V (1967) Oxygen reduction at Pt-Au and Pd-Au alloy electrodes in acid solution. Electrochim Acta 12(9):1171–1184
17. Markovic NM, Adzic RR, Cahan BD, Yeager EB (1994) Structural effects in electrocatalysis – oxygen reduction on platinum low-index single-crystal surfaces in perchloric-acid solutions. J Electroanal Chem 377(1–2):249–259
18. Kondo S, Nakamura M, Maki N, Hoshi N (2009) Active sites for the oxygen reduction reaction on the low and high index planes of palladium. J Phys Chem C 113(29):12625–12628
19. Shao MH, Huang T, Liu P, Zhang J, Sasaki K, Vukmirovic MB, Adzic RR (2006) Palladium monolayer and palladium alloy electrocatalysts for oxygen reduction. Langmuir 22(25): 10409–10415
20. Jalan VM, Luczak FJ, Lee J (1980) US Patent 4192967
21. Landsman DA, Luczak FJ (1982) US Patent 4316944
22. Landsman DA, Luczak FJ (2003) Catalyst studies and coating technologies. In: Vielstich W, Gasteiger H, Lamm A (eds) Handbook of fuel cells, vol 4. Wiley, p 811
23. Jalan V, Taylor EJ (1983) Importance of interatomic spacing in catalytic reduction of oxygen in phosphoric acid. J Electrochem Soc 130:2299
24. Paffett MT, Beery JG, Gottesfeld S (1988) Oxygen reduction at $Pt_{0.65}Cr_{0.35}$, $Pt_{0.2}Cr_{0.8}$ and roughened platinum. J Electrochem Soc 135(6):1431
25. Mukerjee S, Srinivasan S, Soriaga M, McBreen J (1995) Role of structural and electronic properties of Pt and Pt alloys on electrocatalysis of oxygen reduction. J Electrochem Soc 142(5):1409
26. Toda T, Igarashi H, Uchida H, Watanabe M (1999) Enhancement of the electroreduction of oxygen on Pt alloys with Fe, Ni, and Co. J Electrochem Soc 146(10):3750
27. Toda T, Igarashi H, Watanabe M (1998) Role of electronic property of Pt and Pt alloys on electrocatalytic reduction of oxygen. J Electrochem Soc 145(12):4185
28. Paulus UA, Wokaun A, Scherer GG, Schmidt TJ, Stamenkovic V, Markovic NM, Ross PN (2002) Oxygen reduction on high surface area Pt-based alloy catalysts in comparison to well defined smooth bulk alloy electrodes. Electrochim Acta 47(22–23):3787–3798
29. Paulus UA, Wokaun A, Scherer GG, Schmidt TJ, Stamenkovic V, Radmilovic V, Markovic NM, Ross PN (2002) Oxygen reduction on carbon-supported Pt-Ni and Pt-Co alloy catalysts. J Phys Chem B 106:4181
30. Hammer B, Nørskov JK (1995) Electronic factors determining the reactivity of metal surfaces. Surf Sci 343:211
31. Hammer B, Nørskov JK (2000) Theoretical surface science and catalysis calculations and concepts. Adv Catal 45:71
32. Kitchin JR, Nørskov JK, Barteau MA, Chen JG (2004) Role of strain and ligand effects in the modification of the electronic and chemical properties of bimetallic surfaces. Phys Rev Lett 93(15):156801

33. Kitchin JR, Nørskov JK, Barteau MA, Chen JG (2004) Modification of the surface electronic and chemical properties of Pt(111) by subsurface 3d transition metals. J Chem Phys 120(21): 10240
34. Greeley J, Nørskov JK, Mavrikakis M (2002) Electronic structure and catalysis on metal surfaces. Annu Rev Phys Chem 53:319–348
35. Xu Y, Ruban AV, Mavrikakis M (2004) Adsorption and dissociation of O_2 on Pt- Co and Pt-Fe alloys. J Am Chem Soc 126:4714
36. Savadogo O, Lee K, Oishi K, Mitsushima S, Kamiya N, Ota KI (2004) New palladium alloys catalyst for the oxygen reduction reaction in an acid medium. Electrochem Commun 6(2): 105–109
37. Fernandez JL, Raghuveer V, Manthiram A, Bard AJ (2005) Pd-Ti and Pd-Co-Au electrocatalysts as a replacement for platinum for oxygen reduction in proton exchange membrane fuel cells. J Am Chem Soc 127:13100–13101
38. Fernandez JL, Walsh DA, Bard AJ (2005) Thermodynamic guidelines for the design of bimetallic catalysts for oxygen electroreduction and rapid screening by scanning electrochemical microscopy. J Am Chem Soc 127:357–365
39. Fernandez JL, White JM, Sun YM, Tang WJ, Henkelman G, Bard AJ (2006) Characterization and theory of electrocatalysts based on scanning electrochemical microscopy screening methods. Langmuir 22(25):10426–10431
40. Wang W, Zheng D, Du C, Zou Z, Zhang X, Xia B, Yang H, Akins DL (2007) Carbon-supported Pd-Co bimetallic nanoparticles as electrocatalysts for the oxygen reduction reaction. J Power Sources 167(2):243–249
41. Zhang L, Lee K, Zhang JJ (2007) The effect of heat treatment on nanoparticle size and ORR activity for carbon-supported Pd-Co alloy electrocatalysts. Electrochim Acta 52(9):3088–3094
42. Shao MH, Sasaki K, Adzic RR (2006) Pd-Fe nanoparticles as electrocatalysts for oxygen reduction. J Am Chem Soc 128(11):3526
43. Wang RF, Liao SJ, Fu ZY, Ji S (2008) Platinum free ternary electrocatalysts prepared via organic colloidal method for oxygen reduction. Electrochem Commun 10(4):523–526
44. Tarasevich MR, Zhutaeva GV, Bogdanovskaya VA, Radina MV, Ehrenburg MR, Chalykh AE (2007) Oxygen kinetics and mechanism at electrocatalysts on the base of palladium-iron system. Electrochim Acta 52(15):5108–5118
45. Song SQ, Wang Y, Tsiakaras P, Shen PK (2008) Direct alcohol fuel cells: a novel non-platinum and alcohol inert ORR electrocatalyst. Appl Catal B Environ 78(3–4):381–387
46. Xu Y, Shao MH, Mavrikakis M, Adzic RR (2009) Recent developments in the electrocatalysis of the O_2 reduction reaction. In: Koper MTM (ed) Fuel cell catalysis: a surface science approach. Wiley, Hoboken, pp 271–316
47. Sarkar A, Murugan AV, Manthiram A (2009) Low cost Pd-W nanoalloy electrocatalysts for oxygen reduction reaction in fuel cells. J Mater Chem 19:159–165
48. Serov AA, Cho S-Y, Han S, Min M, Chai G, Nam KH, Kwak C (2007) Modification of palladium-based catalysts by chalcogenes for direct methanol fuel cells. Electrochem Commun 9(8):2041–2044
49. Cheng L, Zhang Z, Niu W, Xu G, Zhu L (2008) Carbon-supported Pd nanocatalyst modified by non-metal phosphorus for the oxygen reduction reaction. J Power Sources 182(1):91–94
50. Li H, Sun G, Li N, Sun S, Su D, Xin Q (2007) Design and preparation of highly active Pt-Pd/C catalyst for the oxygen reduction reaction. J Phys Chem C 111(15):5605–5617
51. Guerin S, Hayden BE, Lee CE, Mormiche C, Russell AE (2006) High-throughput synthesis and screening of ternary metal alloys for electrocatalysis. J Phys Chem B 110(29): 14355–14362
52. Ye HC, Crooks RM (2007) Effect of elemental composition of PtPd bimetallic nanoparticles containing an average of 180 atoms on the kinetics of the electrochemical oxygen reduction reaction. J Am Chem Soc 129(12):3627–3633

53. Raghuveer V, Manthiram A, Bard AJ (2005) Pd-Co-Mo electrocatalyst for the oxygen reduction reaction in proton exchange membrane fuel cells. J Phys Chem B 109(48): 22909–22912
54. Mathiyarasuz J, Phani KLN (2007) Carbon-supported palladium-cobalt-noble metal (Au, Ag, Pt) nanocatalysts as methanol tolerant oxygen-reduction cathode materials in DMFCs. J Electrochem Soc 154:B1100–B1105
55. Wang XP, Kariuki N, Vaughey JT, Goodpaster J, Kumar R, Myers DJ (2008) Bimetallic Pd-Cu oxygen reduction electrocatalysts. J Electrochem Soc 155(6):B602–B609
56. Myers DJ (2008) In: DOE hydrogen and fuel cell review meeting, Arlington, VA
57. Raghuveer V, Ferreira PJ, Manthiram A (2006) Comparison of Pd-Co-Au electrocatalysts prepared by conventional borohydride and microemulsion methods for oxygen reduction in fuel cells. Electrochem Commun 8(5):807–814
58. Liu H, Manthiram A (2008) Tuning the electrocatalytic activity and durability of low cost $Pd_{70}Co_{30}$ nanoalloy for oxygen reduction reaction in fuel cells. Electrochem Commun 10(5): 740–744
59. Xiao L, Zhuang L, Liu Y, Lu J, Abruna HD (2008) Activating Pd by morphology tailoring for oxygen reduction. J Am Chem Soc 131(2):602–608
60. Li WZ, Haldar P (2009) Supportless PdFe nanorods as highly active electrocatalyst for proton exchange membrane fuel cell. Electrochem Commun 11(6):1195–1198
61. Shao MH Unpublished data
62. Erikson H, Sarapuu A, Tammeveski K, Solla-Gullon J, Feliu JM (2011) Enhanced electrocatalytic activity of cubic Pd nanoparticles towards the oxygen reduction reaction in acid media. Electrochem Commun 13(7):734–737
63. Shao M, Yu T, Odell JH, Jin M, Xia Y (2011) Structural dependence of oxygen reduction reaction on palladium nanocrystals. Chem Commun 47(23):6566–6568
64. Chierchie T, Mayer C (1988) Voltammetric study of the underpotential deposition of copper on polycrystalline and single crystal palladium surfaces. Electrochim Acta 33(3):341–345
65. Lima FHB, Zhang J, Shao M, Sasaki K, Vukmirovic B, Ticianelli EA, Adzic RR (2007) Catalytic activity-d-band center correlation for the O_2 reduction on Pt in alkaline solutions. J Phys Chem C 111:404–410
66. Arenz M, Schmidt TJ, Wandelt K, Ross PN, Markovic NM (2003) The oxygen reduction reaction on thin palladium films supported on a Pt(111) electrode. J Phys Chem B 107(36): 9813–9819
67. Naohara H, Ye S, Uosaki K (2000) Electrocatalytic reactivity for oxygen reduction at epitaxially grown Pd thin layers of various thickness on Au(111) and Au(100). Electrochim Acta 45(20): 3305–3309
68. Schmidt TJ, Stamenkovic V, Arenz M, Markovic NM, Ross PN (2002) Oxygen electrocatalysis in alkaline electrolyte: Pt(hkl), Au(hkl) and the effect of Pd-modification. Electrochim Acta 47(22–23): 3765–3776
69. Dursun Z, Ulubay Ş, Gelmez B, Ertaş F (2009) Electrocatalytic reduction of oxygen on a Pd ad-layer modified Au(111) electrode in alkaline solution. Catal Lett 132(1):127–132
70. Shao M, Sasaki K, Liu P, Adzic RR (2007) Pd_3Fe and Pt monolayer-modified Pd_3Fe electrocatalysts for oxygen reduction. Z Phys Chem 221:1175–1190
71. Jiang L, Hsu A, Chu D, Chen R (2009) Size-dependent activity of palladium nanoparticles for oxygen electroreduction in alkaline solutions. J Electrochem Soc 156(5):B643–B649
72. Kim J, Park JE, Momma T, Osaka T (2009) Synthesis of Pd-Sn nanoparticles by ultrasonic irradiation and their electrocatalytic activity for oxygen reduction. Electrochim Acta 54(12): 3412–3418
73. Li B, Prakash J (2009) Oxygen reduction reaction on carbon supported palladium-nickel alloys in alkaline media. Electrochem Commun 11(6):1162–1165
74. Nie M, Shen PK, Wei ZD (2007) Nanocrystalline tungsten carbide supported Au-Pd electrocatalyst for oxygen reduction. J Power Sources 167:69–73

75. Lu S, Pan J, Huang A, Zhuang L, Lu J (2008) Alkaline polymer electrolyte fuel cells completely free from noble metal catalysts. Nat Acad Sci Proc 105(52):20611–20614
76. Catanorchi S, Piana M, Gasteiger HA (2008) Kinetics of non-platinum group metal catalysts for the oxygen reduction reaction in alkaline medium. ECS Trans 16(2):2045–2055
77. Mustain WE, Kepler K, Prakash J (2007) CoPdx oxygen reduction electrocatalysts for polymer electrolyte membrane and direct methanol fuel cells. Electrochim Acta 52(5):2102–2108
78. Li HQ, Xin Q, Li WZ, Zhou ZH, Jiang LH, Yang SH, Sun GQ (2004) An improved palladium-based DMFCs cathode catalyst. Chem Commun 23:2776–2777
79. Lopes T, Antolini E, Gonzalez ER (2008) Carbon supported Pt-Pd alloy as an ethanol tolerant oxygen reduction electrocatalyst for direct ethanol fuel cells. Int J Hydrogen Energy 33(20): 5563–5570
80. Lee K, Savadogo O, Ishihara A, Mitsushima S, Kamiya N, Ota K (2006) Methanol-tolerant oxygen reduction electrocatalysts based on Pd-3D transition metal alloys for direct methanol fuel cells. J Electrochem Soc 153(1):A20–A24
81. Mustain WE, Kepler K, Prakash J (2006) Investigations of carbon-supported $CoPd_3$ catalysts as oxygen cathodes in PEM fuel cells. Electrochem Commun 8(3):406–410
82. Tarasevich M, Bogdanovskaya V, Kuznetsova L, Modestov A, Efremov B, Chalykh A, Chirkov Y, Kapustina N, Ehrenburg M (2007) Development of platinum-free catalyst and catalyst with low platinum content for cathodic oxygen reduction in acidic electrolytes. J Appl Electrochem 37(12):1503–1513
83. Wang YX, Balbuena PB (2005) Design of oxygen reduction bimetallic catalysts: ab-initio-derived thermodynamic guidelines. J Phys Chem B 109:18902–18906
84. Fouda-Onana F, Bah S, Savadogo O (2009) Palladium-copper alloys as catalysts for the oxygen reduction reaction in an acidic media I: Correlation between the ORR kinetic parameters and intrinsic physical properties of the alloys. J Electroanal Chem 636(1–2):1–9
85. Rousset JL, Bertolini JC, Miegge P (1996) Theory of segregation using the equivalent-medium approximation and bond-strength modifications at surfaces: application to fcc Pd-X alloys. Phys Rev B 53(8):4947
86. Ruban AV, Skriver HL, Nørskov JK (1999) Surface segregation energies in transition-metal alloys. Phys Rev B 59(24):15990
87. Bozzolo G, Noebe RD, Khalil J, Morse J (2003) Atomistic analysis of surface segregation in Ni-Pd alloys. Appl Surf Sci 219(1–2):149–157
88. Suo YG, Zhuang L, Lu JT (2007) First-principles considerations in the design of Pd-alloy catalysts for oxygen reduction. Angew Chem Int Ed 46(16):2862–2864
89. Shao M, Liu P, Zhang J, Adzic RR (2007) Origin of enhanced activity in palladium alloy electrocatalysts for oxygen reduction reaction. J Phys Chem B 111:6772–6775
90. Zhou W-P, Yang X, Vukmirovic MB, Koel BE, Jiao J, Peng G, Mavrikakis M, Adzic RR (2009) Improving electrocatalysts for O_2 reduction by fine-tuning the Pt-support interaction: Pt monolayer on the surfaces of a $Pd_3Fe(111)$ single-crystal alloy. J Am Chem Soc 131(35): 12755–12762
91. Sasaki K, Shao MH, Adzic RR (2009) Dissolution and stabilization of platinum in oxygen cathodes. In: Buchi FN, Inaba M, Schmidt T (eds) Proton exchange membrane fuel cell durability. Springer, New York, pp 7–28
92. Pourbaix M (1974) Atlas of electrochemical equilibria, 2nd edn. NACE, Houston
93. Wells PP, Crabb EM, King CR, Wiltshire R, Billsborrow B, Thompsett D, Russell AE (2009) Preparation, structure and stability of Pt and Pd monolayer modified Pd and Pt electrocatalysts. Phys Chem Chem Phys 11:5773–5781
94. Zhang J, Vukmirovic MB, Sasaki K, Uribe F, Adzic RR (2005) Platinum monolayer electrocatalysts for oxygen reduction: effect of substrates, and long-term stability. J Serb Chem Soc 70(3):513–525
95. Shao MH, Shoemaker K, Peles A, Kaneko K, Protsailo L (2010) Pt monolayer on porous Pd-Cu alloys as oxygen reduction electrocatalysts. J Am Chem Soc 132(27):9253–9255